UNIVERSITY OF TURIN

&

UNIVERSITÉ PARIS SACLAY

Department of Molecular Biotechnology and Health Sciences

&

Laboratory of Signalling and Cardiovascular Pathophysiology,

Inserm U1180

Joint PhD Program in:

Biomedical Sciences and Oncology (Cycle XXIX)

&

Therapeutic Innovation: from Fundamental to Applied

Speciality: Physiology, Pathophysiology

Cardiac gene therapy with phosphodiesterase PDE4B in a mouse model of heart failure

Jean Piero Margaria

Tutors: Jérôme Leroy
Grégoire Vandecasteele
Prof. Alessandra Ghigo
Thesis Director: Prof. Emilio Hirsch
Thesis Co-Director: Dr. Rodolphe Fischmeister

Academic Years: 2014-2017

Abstract

Activation of the β-adrenergic pathway results in an increase in cAMP which plays a key role in the regulation of cardiac contraction. While an acute stimulation of the β-adrenergic receptors (β-ARs) improves cardiac function, their chronic activation in heart failure (HF) is detrimental to the heart, as it promotes deregulation of intracellular calcium handling and maladaptive remodeling. Multiple phosphodiesterases (PDEs) are responsible for cAMP degradation and compartmentation, and therefore finely tune β-AR responses. We showed previously that PDE4B is decreased in pathological cardiac hypertrophy and PDE4B ablation in mice exacerbates β-AR stimulation of the L-type Ca^{2+} current and the propensity to cardiac arrhythmias. Since long term treatment with PDE inhibitors increases mortality in HF, we hypothesized that decreasing cAMP levels could have a therapeutic effect in this disease.

To address this hypothesis we used two different models: transgenic overexpression of the PDE using the cardiac specific promoter α-MHC, and PDE-encoding adeno-associated virus targeting the heart in adult mice. We explored whether transgenic or serotype 9 adeno-associated viral vectors (AAV9) mediated cardiac overexpression of PDE4B could prevent maladaptive hypertrophy in a mouse model of chronic isoproterenol (Iso) infusion (60 µg/g/day during 2 weeks). Echocardiography allowed cardiac function exploration. PDE4B protein expression in heart extracts was measured by western blot. Heart sections (10 µm thick) were cut from paraffin-embedded specimens and stained with Masson's trichrome to quantify fibrosis.

A ten-fold and five-fold increase in PDE4B protein levels was measured in transgenic and AAV9, respectively. In transgenic mice, constitutive PDE4B overexpression caused a mild hypertrophy in adult mice. In control mice, either wild-type or injected with a AAV9 encoding for Luciferase ($1x10^{12}$ vp), chronic Iso treatment induced cardiac hypertrophy, fibrosis, and decreased ejection fraction (EF) measured by echocardiography. Overexpression of PDE4B did not prevent cardiac hypertrophy induced by Iso, but abolished the increase in fibrosis. More importantly, EF was preserved when PDE4B was overexpressed in this pathological model.

Altogether, these results suggest that gene therapy with AAV9 encoding PDEs is a potential therapeutic approach for cardiac maladaptive hypertrophy.

Riassunto

L'attivazione del pathway β-adrenergico determina un aumento del cAMP che svolge un ruolo chiave nella regolazione della contrazione cardiaca. Mentre una stimolazione acuta dei recettori β-adrenergici (β-AR) migliora la funzione cardiaca, la loro attivazione cronica nell'insufficienza cardiaca (IC) è dannosa per il cuore, in quanto promuove la deregolazione del calcio intracellulare e il rimodellamento maladattativo. Le fosfodiesterasi (PDEs) sono responsabili della degradazione e compartimentazione del cAMP e quindi regolano finemente le risposte β-AR. Abbiamo dimostrato in precedenza che la PDE4B è diminuita nell'ipertrofia cardiaca patologica e l'ablazione della PDE4B nei topi esacerba la stimolazione β-AR della corrente di Ca^{2+} tipo L e la propensione alle aritmie cardiache. Poiché il trattamento a lungo termine con inibitori delle PDE aumenta la mortalità nell'IC, abbiamo ipotizzato che la riduzione dei livelli di cAMP potrebbe avere un effetto terapeutico in questa malattia.

Abbiamo esplorato se la sovraespressione cardiaca mediante un sistema trasgenico o con vettori virali adeno-associati sierotipo 9 (AAV9) di PDE4B potrebbe prevenire l'ipertrofia maladattativa in un modello murino di infusione cronica di isoproterenolo (Iso) (60 μg / g / giorno per 2 settimane). L'ecocardiografia ha consentito l'esplorazione della funzione cardiaca. L'espressione della proteina PDE4B negli estratti cardiaci è stata misurata mediante western blot. Sezioni di cuore (spessore 10 μm) sono state tagliate da campioni inclusi in paraffina e colorate con tricromia di Masson per quantificare la fibrosi.

Un aumento di dieci volte e di cinque volte dei livelli di proteina PDE4B è stato misurato rispettivamente nei transgenici e AAV9. Nei topi transgenici, la sovraespressione costitutiva della PDE4B ha causato una lieve ipertrofia cardiaca nei topi adulti. Nei topi di controllo, wild type o iniettati con AAV9 codificante per la Luciferasi ($1x10^{12}$ particelle virali), il trattamento cronico con Iso ha indotto ipertrofia cardiaca, fibrosi e riduzione della frazione di eiezione (EF) misurata mediante ecocardiografia. La sovraespressione di PDE4B non ha impedito l'ipertrofia cardiaca indotta dall'Iso, ma ha abolito l'aumento della fibrosi. Inoltre, l'EF è rimasta invariata quando PDE4B è stato sovraespresso in questo modello patologico.

Complessivamente, questi risultati suggeriscono che la terapia genica con AAV9 codificante per PDE è un potenziale approccio terapeutico per l'ipertrofia cardiaca maladattativa.

Résumé

L'activation de la voie β-adrénergique entraîne une augmentation de l'AMPc qui joue un rôle clé dans la régulation de la contraction cardiaque. Alors qu'une stimulation aiguë des récepteurs β-adrénergiques (β-AR) améliore la fonction cardiaque, leur activation chronique dans l'insuffisance cardiaque (IC) est préjudiciable au cœur, car elle favorise la dérégulation du calcium intracellulaire et le remodelage pathologique du cœur. Les phosphodiestérases (PDE) sont responsables de la dégradation de l'AMPc et de la compartimentation, et donc ajuste nt finement les réponses β-AR. Nous avons montré précédemment que la PDE4B est diminuée dans l'hypertrophie cardiaque pathologique et que l'ablation de PDE4B chez la souris exacerbe la stimulation β-AR du courant Ca^{2+} de type L et la propension aux arythmies cardiaques. Étant donné qu'un traitement à long terme par des inhibiteurs de la PDE augmente la mortalité dans l'HF, nous avons supposé que la diminution des taux d'AMPc pourrait avoir un effet thérapeutique dans cette maladie.

Nous avons exploré si la surexpression cardiaque médiée par les vecteurs viraux adéno-associés sérotype 9 (AAV9) ou à l'aide d'un système transgénique de PDE4B pourrait prévenir une hypertrophie dans un modèle murin d'infusion chronique d'isoprotérénol (Iso) (60 μg / g / jour pendant 2 semaines). L'échocardiographie a permis l'exploration de la fonction cardiaque. L'expression de la protéine PDE4B dans les extraits de coeur a été mesurée par western blot. Des coupes de cœur (10 μm d'épaisseur) ont été prélevées sur des échantillons inclus en paraffine et colorées avec le trichrome de Masson pour quantifier la fibrose.

Une augmentation de dix fois et cinq fois des niveaux de protéines PDE4B a été mesurée dans les transgéniques et les AAV9, respectivement. Chez les souris transgéniques adulte, la surexpression constitutive de la PDE4B a provoqué une légère hypertrophie. Chez les souris témoins, de type sauvage ou ayant reçu un AAV9 codant pour la Luciferase($1x10^{12}$ particules virales), le traitement par Iso chronique a induit une hypertrophie cardiaque, une fibrose et une diminution de la fraction d'éjection (EF) mesurée par échocardiographie. La surexpression de PDE4B n'a pas empêché l'hypertrophie cardiaque induite par Iso, mais a aboli l'augmentation de la fibrose. Plus important encore, l'EF a été préservé lorsque PDE4B a été surexprimé dans ce modèle pathologique.

Au total, ces résultats suggèrent que la thérapie génique avec des AAV9 codant pour PDE est une approche thérapeutique potentielle pour le traitement de l'hypertrophie cardiaque inadaptée.

Introduction

Isoproterenol-induced heart failure

Heart failure (HF) incidence is growing worldwide, primarily due to the overall aging of the population and to the diffusion of cardiovascular risk factors, such as diabetes, hypertension, overweight, dyslipidemia, and physical inactivity. Classic treatments for HF are neuroendocrine antagonists, digitalis, and diuretics, which have contributed to ameliorate the outcomes of HF patients in the last decades. In particular typical treatment of HF with reduced ejecton fraction (HFrEF) are angiotensin-converting enzyme inhibitors (ACEI), beta-blockers, and mineralocorticoid/aldosterone receptor antagonists (MRAs). Alternative and additional treatments are diuretics, angiotensin receptor neprilysin inhibitor (ARNI), ivabradine, angiotensin II type I receptor blockers (ARBs), and combination of hydralazine and isosorbide dinitrate, depending on the specific condition of the patient[1]. While HFrEF strongly responds to standard treatments for HF, HF with preserved ejection fraction (HFpEF) appears more refractory to traditional approaches and is usually treated with diuretics to improve congestion[1]. Despite consolidated standard treatment, HF is still associated with high mortality, reduced quality of life, and repeated hospitalizations.

The current animal models of HF are divided in the following classes: surgical, genetic and toxin-induced models. First, among the surgical models, transverse aortic constriction (TAC) and permanent ligation of the left anterior descending artery (LAD) to mimic myocardial infarction are frequently used to resemble the specific human disease situation[2]. Secondly, over 5000 genetic models of HF (mainly cardiac transgenic/knockout animals) have been employed and proven to be essential to study specific signaling pathways. The latter are toxin-induced models, including doxorubicin and isoproterenol, which are used in mice to induce heart failure syndrome. In particular isoproterenol stimulation mimics cardiotoxic effects of chronic activation of the sympathetic system[3].

The choice of the right animal model depends on the scientific purpose and can only address part of the complexity of the clinical HF syndrome. Especially isoproterenol stimulation represents the best way to study β-adrenergic pathway in the heart and elevated circulating catecholamines produced to counteract decreased cardiac output in HF.

Phosphodiesterases

The scope of this work is to investigate whether phosphodiesterase 4B (PDE4B) overexpression in the heart is able to modulate the physiological and pathological cardiac behavior. Cyclic nucleotide phosphodiesterases (PDEs) are a superfamily of enzymes that catalyze the hydrolysis of the cyclic adenosine monophosphate (cAMP) and cyclic guanosine monophosphate (cGMP), to adenosine monophosphate (AMP) and guanosine monophosphate (GMP), respectively. Cyclic nucleotides are produced in intracellular microdomains where they are catabolized by specific PDEs[4]. The superfamily is encoded by 21 genes divided

in 11 families responsible for the termination of cyclic nucleotide signaling. Each family displays different kinetic parameters and specifically hydrolyze cAMP (families PDE4, 7, and 8), cGMP (families PDE5, 6, and 9), or both cAMP and cGMP (families PDE1, 2, 3, 10, and 11).

During the β-adrenergic stimulation, the adrenergic receptor is responsible for the activation of adenylate cyclases which in turn synthetize cAMP. Cyclic nucleotides, catabolized by PDEs, regulate different molecular targets such as cAMP activated protein kinase A (PKA), protein kinase G (PKG), Rap guanine nucleotide exchange factor 3 (EPAC) and cyclic nucleotide-gated channels (CNG)[5,6]. Among these targets the most studied is PKA, a protein kinase activated by cAMP, which is able to phosphorylate multiple downstream effectors important for excitation contraction coupling in cardiomyocytes: the L-type calcium channel ($Ca_v1.2$), the ryanodine receptor (RyR2), and the SERCA2 inhibitory protein phospholamban (PLB)[7]. Given the role of PDEs in hydrolyzing the cyclic nucleotides, the modulation of cAMP degrading PDEs can impact on excitation contraction coupling in cardiomyocytes and on cardiac function.

PDEs and cardiac function regulation

PDEs hydrolyzing cAMP expressed in the heart are only five: PDE1, PDE2, PDE3, PDE4 and PDE8. Every phospohodisterase family display different regulatory domains, PDE1 is regulated by Calmodulin, PDE2 is activated by cGMP which binds its GAF domains, PDE3 is inhibited by cGMP, and PDE4 is modulated by phosphorylation on its UCR domains[8]. Previous studies, in particular on PDE4 family using knockout mice have provided a valuable insight on their intracellular function. In particular PDE4A, PDE4B and PDE4D have been knocked-out in the laboratory of Marco Conti and each of these genes have been shown to play a non-redundant regulatory role which is not compensated by the presence of the other three very similar PDE4 genes[9–12]. Moreover each one of the PDE4 genes displays a number of splicing variants, which differs for their N-terminal region encoding regulatory domains and phosphorylation sites, therefore it is not difficult to imagine how every variant can differ from the others in its regulatory mechanisms and cellular localization[8]. As an example in the mouse there are five different splicing variants of the Pde4b gene (https://www.ncbi.nlm.nih.gov/gene/18578), the longest variant is named isoform 1 and is the one used in the present study, while the other variants show different N-terminal regions thus involving changes in intracellular regulation and localization. The two phosphodiesterases that account for the major cAMP hydrolyzing activity in the heart are PDE3 and PDE4. Milrinone, a PDE3 inhibitor, has been shown to have deleterious effects in chronic heart failure patients[13], thus an overexpression of this enzyme could invert these effects. PDE3 is encoded by 2 genes (PDE3A and PDE3B), where PDE3A is the most expressed in rat cardiomyocytes[14,15]. Previous studies from our laboratory demonstrate that among the four PDE4 family genes, PDE4A, PDE4B and PDE4D are expressed in mouse heart tissue and account for one third of the total PDE4 activity each[16].

Importantly hypertrophied myocytes, in a compensated hypertrophy in a rat TAC model, show reduced PDE4-mediated cAMP degradation, in particular because of a downregulation of PDE4B[17]. In addition to this potential role in the hypertrophic process, PDE4B regulates Ca^{2+} homeostasis and associates with the L-type Ca^{2+} channel complex and its invalidation promotes ventricular arrhythmias[16,18,19].

In summary, PDE4B could play a protective role in heart by modulating Ca^{2+} current, and may have a role in hypertrophy progression of cardiomyocytes. Therefore, overexpressing PDE4B could represent a strategy to treat cardiomyopathies through Ca^{2+} current regulation and β-adrenergic stimulation blunting.

Results

Cardiac phenotype of PDE4B transgenic mice

To gain insights into the role of PDE4B in controlling cardiac function, transgenic mice with cardiomyocyte specific expression of the longest splicing isoform, PDE4B1, under the control of the rodent alpha-myosin heavy chain (α-MHC) promoter were generated. We selected a mouse line with moderate PDE4B overexpression. In TG heart tissue, a significant eighty fold increase in mRNA encoding PDE4B and a nine fold increase in protein expression were found compared to matched wild type mice (Figure 1A-B). Transgenic expression of PDE4B was translated in a seven fold elevation of total cAMP-PDE activity in cardiac tissue, supporting the presence of an active PDE produced by the transgenic DNA fragment (Figure 1C). Consistent with the elevated cAMP degradation, basal concentration of the cyclic nucleotide was found decreased by 30% in the heart collected from TG mice (Figure 1D). However, the level of expression of the main PDE isoforms expressed in heart, PDE3A, PDE3B, PDE4A and PDE4D remained unchanged in TG indicating that no compensatory downregulation of their expression took place in the heart of these animals (Supplemental Figure 1A-C).

To evaluate the consequences of the PDE4B overexpression on cardiac function, we performed echocardiographic and anatomical analysis. While heart rate remained unchanged, the heart contractility quantified as fractional shortening, was found significantly decreased from 68.4% in WT to 51.3% in TG mice (Figure 1E). This is in line with the reduced basal cAMP in PDE4B transgenic mice and with the fact that PDE4B overexpression may counteract the predominant sympathetic tone in mice. A trend for increase in left ventricle diastolic diameter (3.9 *vs* 4.17 mm) and weight (98.6 *vs* 113 mg) measured by echocardiography was found in TG but did not reached statistical significance (Figure 1E). However, anatomical analysis revealed a mild hypertrophy in PDE4B TG mice, while reduced fractional shortening did not affect fluid retention in lungs, as shown by the unchanged lungs weight (Figure 1F). Consistent with this hypertrophy, ANP and BNP were increased but not collagen gene expression (data not shown), suggesting that this is rather a compensatory hypertrophy consequent to the diminished fractional shortening than a maladaptive hypertrophy.

Altogether these results point out the consequences of increased PDE4B activity on cAMP degradation and basal levels in mice heart resulting in a decreased cardiac output. Furthermore, our results suggest that a compensatory mild myocardial hypertrophy in PDE4B-TG mice took place which was not maladaptive as attested by the fact that heart function does not worsen with time, do not die prematurely (Supplemental Figure S2A-C), have normal exercise capacity and exhibited an increased endurance distance of treadmill running to exhaustion (Supplemental Figure S3C). However, this is not the case for mice from a line expressing 40 times more PDE4B protein and in which cAMP-PDE is increased by more than 50 (Supplemental Figure S5A-E). These mice fractional shortening and cardiac hypertrophy are drastically altered and get worse with time, leading to early death of the mice

(Supplemental Figure S2A-C).

PDE4B overexpression blunts β-AR stimulation of heart function

To better characterize intrinsic contractile properties of TG mice hearts, these organs were explanted to evaluate their function *ex vivo*. As previously highlighted *in vivo* by echocardiography, heart rate was unaffected by PDE4B overexpression, eluding any compensatory neurohormonal mechanism counteracting PDE4B overexpression effects on cardiac frequency in vivo (Figure 2A). This has been further corroborated by ECGs recorded in freely moving unrestrained mice, since heart rate remained unchanged across circadian rhythm compared to WT animals (Supplemental Figure S3A). However, upon β-AR stimulation with Isoproterenol (Iso), while heart rate of WT and TG mice was increased, these chronotropic effects were dampened in mice overexpressing PDE4B (Supplemental Figure S3B), suggesting that this enzyme might be a secondary controller of heart rate. Developed pressure was found unaltered under basal conditions, revealing preserved contractile capacities of TG hearts (Figure 2A). However, upon β-AR stimulations, isolated TG hearts were less responsive to submaximal concentrations of Iso (Figure 2B), but developed pressure in TG hearts was equivalent to that of WT upon high agonist concentrations. Dose response curves for the effect of the agonist on developed pressure revealed an expected shift to the right thus an increased EC50 (Figure 2B). These results are indicative of a diminished efficiency of the β-AR agonist to produce inotropic effects due to the increase in cAMP degradation as found *in vivo* (Supplemental Figure S4A-D). They are consistent with a lower response to physiological catecholamine concentrations of PDE4B-TG hearts rather than a decrease of their intrinsic contractile capacities.

PDE4B overexpression decreases intracellular cAMP levels and PKA activity upon β-AR stimulation, leading to blunted stimulation of excitation-contraction coupling and pro-arrhythmic effects of isoproterenol

To investigate at the cellular level how PDE4B increased expression affects the β-AR signaling pathway controlling cardiac function, intracellular cyclic AMP concentration and PKA activity were monitored using FRET biosensors EPAC-S^{H187} [20] and AKAR3-NES[21] respectively. While a brief application of ISO (30 nmol/l, 15s) produced a clear increase of 177% of the CFP/YFP ratio in WT cells expressing EPAC-S^{H187}, it only reached 35% in TG cells (Figure 3A). Similarly, the same Iso application increased the PKA activation measured by FRET ratio only by 15% in TG cells compared to 53% in WT cells (Figure 3B). As a result of the increased PDE4B activity, the β-AR stimulation of the L-type Ca^{2+} current ($I_{Ca,L}$) was also severely blunted, diminishing the potentiation of the Ca^{2+} entry in the cardiomyocyte by three fold upon a brief stimulation of Iso (30 nM, 15 s), suggesting a diminished PKA phosphorylation of the channel (Figure 3C). All these reduced effects of Iso were due to PDE4B overexpression, not to a downregulation of the β-AR signaling pathway since upon PDE4 inhibition with Ro2017-24 (10 µM) application the β-AR agonist led to similar increases of cAMP and PKA activity and $I_{Ca,L}$ amplitude in either WT or TG cardiomyocytes (Supplemental Figure S4A-D). To further investigate the PKA

downstream signaling of the β-AR pathway, phosphorylated targets were quantified by analyzing ventricular protein extracts. Phosphorylation of phospholamban (PLB), troponin I (TnI), and myosin binding protein C (MyBPC) at PKA specific sites (and CaMKII *i.e* Thr17 site for PLB) was significantly diminished in cardiac tissues obtained from PDE4B-TG mice (Figure 3D-F) demonstrating decreased PKA (and CaMKII) activity. Accordingly, Ca^{2+} transient and sarcomere shortening amplitudes measured simultaneously in isolated ventricular myocytes revealed an attenuation of the inotropic and lusitropic effects (consistent with a decreased cytosolic Ca^{2+} uptake in PDE4B-TG myocytes) of a β-AR stimulation by Iso even at high concentration (100 nM), whereas basal contractility and Ca^{2+} transients were similar between WT and PDE4B-TG mice (Figure 4A-F). Again, these effects were normalized by PDE4 inhibition demonstrating that their reduction was actually due to increased PDE4 activity. These results are in line with the unaltered contractile properties and the diminished response to the β-AR agonist of cardiac ventricular function evaluated *in vivo* or *ex vivo*. Furthermore, while about 80% of isolated WT ventricular myocytes exposed to Iso (100 nM) showed frequent occurrences of spontaneous Ca^{2+} waves (SCWs), SCWs were nearly abrogated in myocytes isolated from PDE4B-TG mice with less than one spontaneous event triggered by less than 50 % of the cardiomyocytes (Figure 4G-I). Thus, PDE4B overexpression protects cardiomyocytes from these pro-arrythmogenic events triggered by β-AR stimulation.

PDE4B overexpression protects from maladaptive remodeling induced by chronic infusion of isoproterenol

To determine the potential protective effects of the overexpression of PDE4B under stress conditions, mice were subjected to chronic Iso infusion (60 mg/Kg/day) for two weeks and cardiac function was evaluated by echocardiography on the day of the osmotic minipump implantation, at the end of the 2 weeks treatment and before sacrifice 4 weeks later (Figure 5A). Heart weight was measured at the time of sacrifice (Figure 5B) revealing a significant hypertrophy induced by Iso in WT mice compared to NaCl treated mice, while only a trend to increased cardiac mass was observed in PDE4B-TG mice (Figure 5B). Moreover, Iso led also to an increased lung weight in WT mice but not in PDE4B-TG animals (Figure 5C). Furthermore, Masson's trichrome staining revealed an increase of cardiac fibrosis in the left ventricle in WT subjected to Iso, whether PDE4B-TG mice appeared protected (Figure 5D,H). Together, these results suggest a maladaptive remodeling and an impaired heart function leading to congestion in WT but not in PDE4B-TG mice, which seems to be protected. Accordingly, echocardiography revealed a decreased fractional shortening two weeks after the beginning of the treatment and 4 weeks after, while cardiac function was first increased then preserved in 4BTG-Iso mice compared to NaCl treated animals (Figure 5D,E and Supplementary Table 1). Hypertrophy of the left ventricle was also confirmed, appearing as soon as after two weeks of treatment in WT mice, while it was not observed in PDE4B-TG mice treated by Iso compared to NaCl treated animals (Figure 5F and Supplementary Table 1). Both WT and PDE4B-TG mice infused with Iso displayed an increase in heart rate two weeks

after the beginning of the treatment, while resting heart rate was restored in all the conditions once the β-AR agonist diffusion ended, attesting that all groups were accordingly treated (Figure 5G and Supplementary Table 1). To further examine the potential therapeutic effects of amplified PDE4B activity in the heart, adeno-associated virus type 9 (AAV9) were engineered to express the PDE coding sequence fused with a FLAG-tag to the N-terminal region, while a second virus encoding luciferase(Luc) gene was used as control (Supplementary Fig S6A). Mice were first injected with 10^{12} vp of AAV9 encoding either PDE4B or Luc, 2 weeks prior minipump implantation (Figure 6A), leading to a fyve fold increase of PDE4B protein in ventricular tissue (Supplementary Fig S6B). However, in contrast to what was observed in PDE4B-TG mice, this mild overexpression of PDE4B did not decrease fractional shortening (Supplementary Fig S6C), probably because this approach only slightly increased PDE4 activity and elevated by only 1.5 fold the cAMP degrading PDE activity (Supplementary Fig S6D). While gene therapy with PDE4B could not fully prevent the increase in heart weight induced by Iso (Figure 6B), similarly to what was observed in PDE4B-TG mice, it prevented the fibrosis(Figure 6D, H). Strikingly, the decrease in fractional shortening induced by chronic Iso infusion observed in animals overexpressing Luc, was absent from animals injected with the AAV9-PDE4B (Figure 6E) which were also partially protected against the increase in left ventricular mass (Figure 6F). Similarly to transgenic mice, increased heart rate upon Iso treatment was observed in AAV9-Luc and AAV9-PDE4B injected mice (Figure 6G). In summary, overexpression of PDE4B partially prevents maladaptive remodeling but more importantly, protects the heart against the cardiac dysfunction induced by chronic isoproterenol infusion stimulation.

Discussion

The present study demonstrates that mild overexpression of PDE4B, a cAMP degrading phosphodiesterase, do not alter cardiac physiological parameters in a maladaptive manner in healthy mice, while at the same time protects against catecholamine induced heart failure. β-blockers are used in the classical treatment of heart failure and have shown to be highly effective in the treatment of abnormal heart rythms and to protect heart from second heart attack. However many adverse effects are associated with the use of these compounds including nausea, diarrhea, bronchospasm, dyspnea, bradycardia, hypotension, heart failure, heart block, and fatigue. Therefore an alternative treatment could be represented by blunting the β-adrenergic signaling downstream in the cascade, possibly maintaining the beneficial effect and excluding the adverse ones by targeting specific and localized pools of cAMP. The PDEs superfamily represents an outstanding toolkit to face this challenge.
Despite extensive studies in the last 30 years focused on inhibition of PDEs and their therapeutic potential on cardiomyopathies, little is known on the consequences of their overexpression in animal models. Only the phosphodiesterase PDE2A has been already overexpressed in heart tissue and has been shown to be protective against catecholamine-induced arrhythmia and to preserve heart function after myocardial infarction[22]. This study provides key advances in the current knowledge of cAMP and Ca^{2+} signaling blunting upon cardiac PDE4B overexpression both *in vitro* and *in vivo*.
Among the PDE4 family, PDE4B is responsible for one third of the PDE4-mediated cAMP degradation in cardiomyocytes[16]. Previous study from our laboratory show that reduction of cardiac PDE4B in a context of isoproterenol stimulation and ventricular burst pacing triggers ventricular tachycardia[16]. Here, we provide evidence that transgenic overexpression of PDE4B ensures protection against arrhythmic events in isolated cardiomyocytes, and this result should be proven *in vivo* to assess whether this effect is also true in the complete organ. Although PDE4B expression is diminished in heart extract from hypertrophied cardiomyocytes suggesting a causal role of PDE4B in the process[17], PDE4B transgenic mice develop cardiac hypertrophy under physiological condition. We do not observe development of hypertrophy in AAV9 treated mice, where the expression is induced in adult mice, after eight weeks of overexpression. This difference can be explained by the role played by the cAMP in the early cardiac development in PDE4B transgenic mice, which has been shown to impair a correct organ formation[23]. Cardiac hypertrophy is accompanied by a decreased ejection fraction, which is in line with a strong cAMP hydrolysis, subsequent decrease in PKA phosphorylation cascade leading to the reduced cardiomyocytes contractility that we observed. ANP and BNP are increased, consistent with the observed hypertrophy, but not collagen gene expression, pointing out a condition attributable to physiological remodeling of the muscle in consequence of reduced ejection fraction rather than a pathological condition. Indeed heart function does not aggravate during the eight weeks follow-up. Furthermore mice show normal exercise activity and display enhanced endurance distance of treadmill running to exhaustion. This result is particularly important in comparison to classical treatments,

in the sense that we observed a blunted cAMP production in concomitance with an increased physical endurance, and this behavior is different from β-blockers which blunt cAMP but cause the adverse effect of fatigue. Nevertheless, mice from a line expressing 40 times more PDE4B protein are strongly impaired in their cardiac function, and their fractional shortening and cardiac hypertrophy get worsen over time, eventually causing premature death. This scenario underlines an overexpression window of PDE4B in which there is a physiological cardiac remodeling, and another one in which the amount of the phosphodiesterase is too elevated and may cause cardiac developmental impairment and detrimental effects in cardiac function and viability.

Isoproterenol stimulation on isolated heart is able to produce an inotropic effect which is mediated by cAMP production through β-AR stimulation. Here we show that an increase in PDE4B counteract Isoproterenol inotropic effect by enhancing cAMP degradation.

Isoproterenol chronic stimulation induce a cardiomyopathy characterized by cardiac hypertrophy, decreased ejection fraction, lung congestion, and cardiac fibrosis[2,24]. PDE4B overexpression either by transgenic or AAV9 mediated expression protects the heart from maladaptive remodeling by reducing detrimental effects on ejection fraction, cardiac fibrosis and lung congestion. We observe the same increase in heart rate in WT and PDE4B overexpressing mice, both AAV9 and transgenic, suggesting either that the concentration of isoproterenol released by the minipumps is too high to highlight a difference in this parameter, or that PDE4B is not overexpressed in the sinus node where it could have an effect on the heart rhythm regulation.

The Luciferase gene has been shown to trigger immune response in mice[25]. Despite we didn’t see leukocytes infiltration in heart slices derived from AAV9-Luc mice, the study could be repeated by using empty AAV9 instead of Luciferase expressing AAV9, in order to avoid a contribution from the immunological system in the pathological model.

In summary, we show for the first time a partial prevention of maladaptive remodeling upon overexpression of PDE4B but more importantly, a protection against the cardiac dysfunction induced by chronic isoproterenol infusion stimulation. The next step will be to test whether the increase in PDE4B can be effective in other models of cardiomyopathy. The most suitable approaches to mimic a the human pathological condition are TAC and MI models. Contrary to the transgenic mice, the AAV9 approach will allow to test both the preventive and therapeutic effect of PDE4B overexpression, and understand whether the loss of cAMP compartmentalization seen in heart failure is a reversible process.

Figures

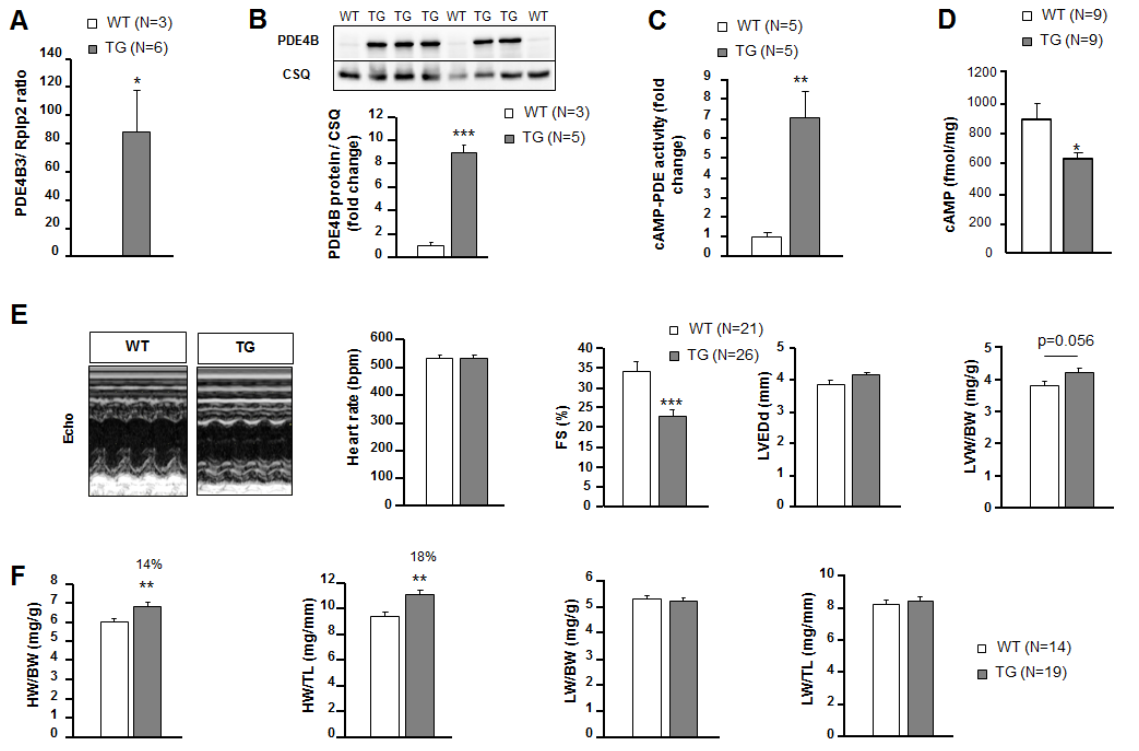

Figure 1

Figure 1: Cardiac phenotype of transgenic 8-10 weeks old mice with cardiac specific PDE4B overexpression.

A, PDE4B1 mRNA expression in WT and PDE4B-TG heart extracts measured by qRT-PCR. (n≥3 per group) **B**, PDE4B protein expression in heart extracts from WT and PDE4B-TG mice measured by Western blot. (n≥3 per group) Calsequestrin (CSQ) is used as normalizer. **C**, PDE activity in heart extracts from WT and PDE4B-TG mice was measured by PDE assay using 1 µM cAMP as a substrate. (n=5 per group) **D**, cAMP levels measured in extracts obtained from WT and PDE4B-TG hearts. (n=9 per group) **E**, Representative images, heart rate, Fractional shortening (FS), left ventricle end diastolic diameter (LVEDd) and left ventricular weight (LVW) evaluated by echocardiography on anesthetized mice and normalized to body weight (BW). (n≥21 per group) **F**, Mean of measured heart weight (HW) and lung weight (LW) normalized to tibia length (TL) or body weight (BW). (n≥14 per group) Statistical significance was determined by student T-test (**P*<0.05, ***P*<0.01, ****P*<0.001).

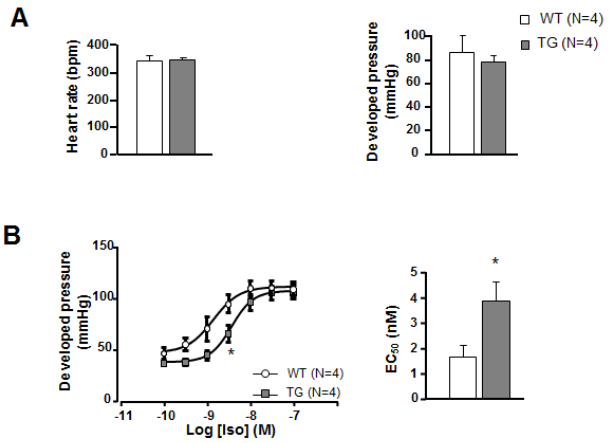

Figure 2

Figure 2: Cardiac function and inotropic β-AR responses measured in isolated hearts from WT and PDE4B-TG mice.

A, Heart rate and developed pressure were measured in Langendorff perfused hearts at baseline. (n=4 per group) **B**, Concentration-response curves of isoprenaline (Iso) on developped pressure measured on WT and PDE4B-TG hearts paced at 650 bpm. EC50 deduced from these curves are reported. (n=4 per group) Statistical significance was determined by student T-test and Two-Way ANOVA (*P<0.05).

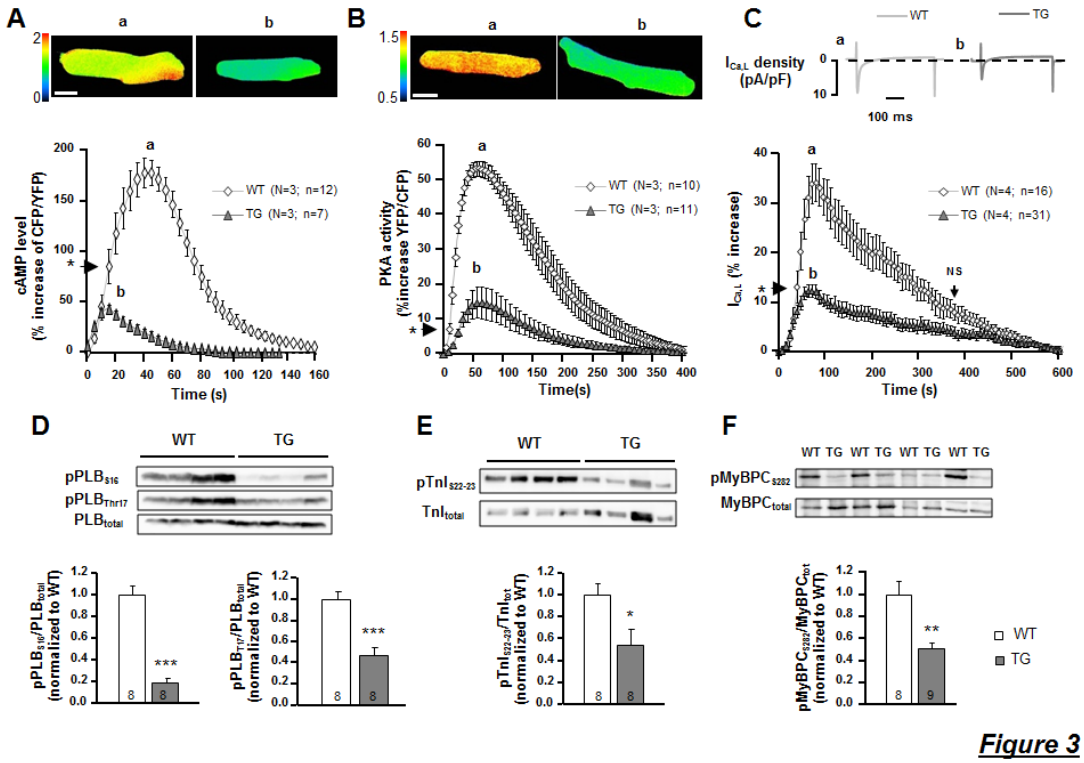

Figure 3

Figure 3: Overexpression of PDE4B decreases cAMP levels, PKA activity and L-type Ca^{2+} channel current amplitude upon β-AR stimulation measured in ventricular cardiomyocytes and the phosphorylation of key proteins of ECC in ventricular tissue.

A, **B**, Normalized average time course of cAMP level and PKA activity measured in response to a 15-second application of Isoproterenol (Iso) (30 nM) in wild-type (WT) and PDE4B-TG ventricular myocytes transduced for 24 h with adenoviruses encoding either the FRET (Förster Resonance Energy Transfer)-based cAMP sensor EPAC-SH[187] or the FRET based PKA activity reporter AKAR3-NES. Representative pseudocolor images of CFP/YFP or YFP/CFP ratio recorded at the time indicated by the letters on the graphs for WT and TG (upper panel) are represented. **C**, Mean variation of $I_{Ca,L}$ amplitude following Iso application (30nM, 15 s). The individual current traces shown on top were recorded at the times indicated by the corresponding letters in the graph below. **D-F**, Whole proteins were extracted from WT and PDE4B-TG mice cardiac ventricles and analyzed by western blot using antibodies for phospho-PLB (P-PLB) (**D**), phospho-TnI (P-TnI) (**E**), phospho-myosin-binding protein C (P-MyBP-C) (**F**). Representative blots are shown, and phosphorylated proteins/total proteins ratios were quantified and expressed as means ± SEM. Graphs represent the mean ± SEM.

Statistical significance was determined by student T-test and Two-Way ANOVA (*P<0.05, **P<0.01, ***P<0.001).

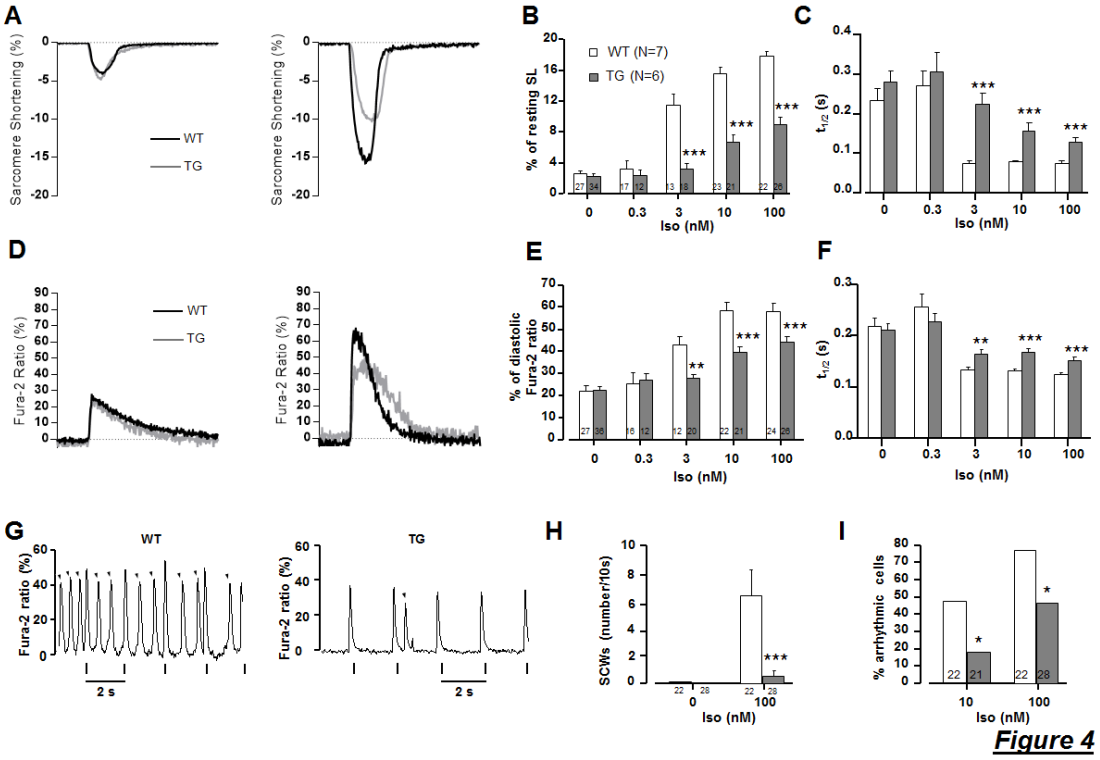

Figure 4: myocardium Ca^{2+} transient amplitude and sarcomere shortening are preserved under basal conditions in isolated ventricular cardiomyocytes from PDE4B-TG mice while the inotropic, lusitropic and pro-arrhythmic effects of Iso are blunted.

A, Representative traces of sarcomere shortening recorded in electrically paced (0.5 Hz) ventricular myocytes isolated from WT (black traces), PDE4B-TG mice (grey traces) in control conditions (left panel) and when the maximal effect produced by isoproterenol (100 nM) was reached (right panel). **B**, Mean data for sarcomere shortening (expressed as the percentage of resting length); (n≥6 per group) **C**, Average $t_{1/2}$ values for sarcomeres relaxation; (n≥6 per group) **D**, Representative traces of Ca^{2+} transients recorded in electrically paced (0.5 Hz) ventricular myocytes isolated from WT (black traces), PDE4B-TG mice (grey traces) in control conditions (left panel) and when the maximal effect produced by isoproterenol (Iso)(100 nM) was reached (right panel). **E**, Fura-2 ratio (expressed as the percentage of diastolic ratio) variation; (n≥6 per group) **F**, Average $t_{1/2}$ values for Ca^{2+} transient return to diastolic levels, measured in control conditions (white bars) and at the maximum of increasing doses of Iso (gray). (n≥6 per group) **G**, Representative traces of spontaneous Ca^{2+} events

(SCWs, arrows) induced by Iso (100 nM) in a WT and a PDE4B-TG cardiomyocytes paced at 0.5 Hz. **H**, Bar graph representing the average number of SCWs during a 10 second period after the peak of the Iso effect in WT (White) and PDE4B-TG (gray). (n≥21 per group) **I**, The percentage of cells exhibiting these pro-arrhythmic events. (n≥21 per group) Graphs represent the mean ± SEM. Statistical significance was determined by Two-Way ANOVA (*P<0.05, **P<0.01, ***P<0.001).

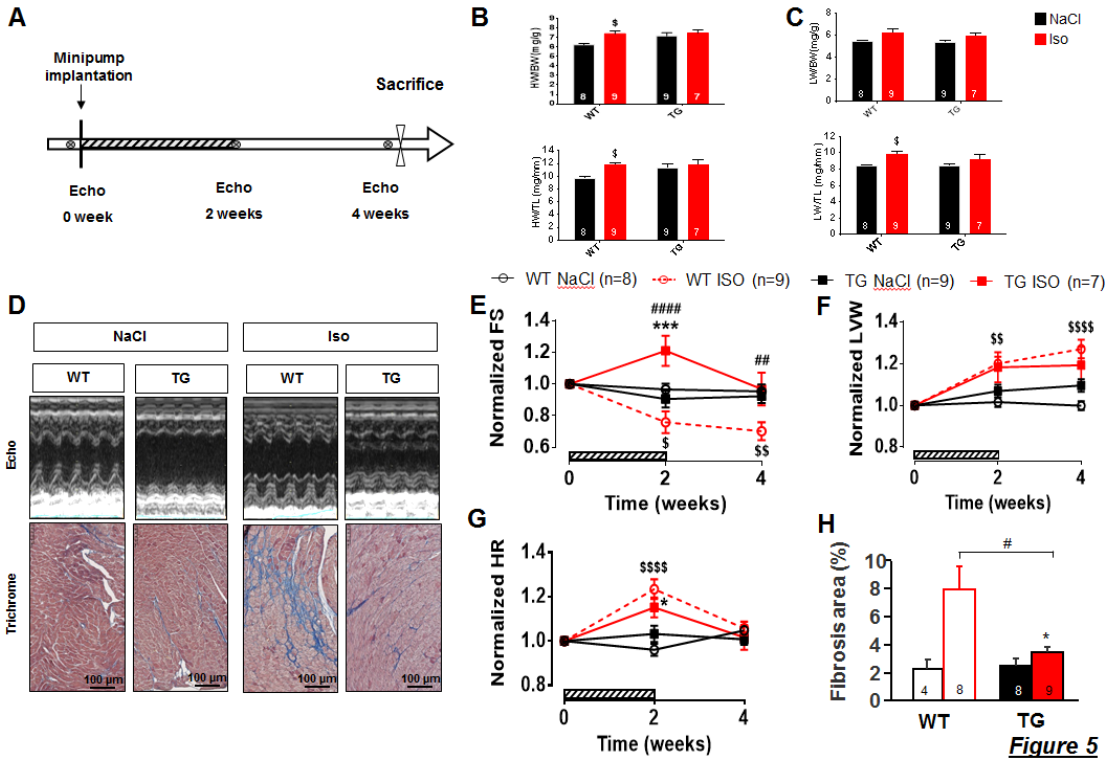

Figure 5: PDE4B-TG mice are protected against maladaptive remodeling induced by chronic infusion with isoproterenol.

A, Schematic representation of the isoproterenol (Iso) treatment protocol. Mice were implanted subcutaneously with osmotic minipumps diffusing 60 mg/Kg/day of Iso or vehicle solution (0.9% NaCl) during 2 weeks (hatched bars). They were kept alive for two additional weeks prior sacrifice. Cardiac function was evaluated by echocardiography before, 2 and 4 weeks after the minipump implantation. **B** and **C**, Bar graphs correspond to the mean heart (HW) and lung weight (LW) of WT mice and PDE4B-TG which underwent NaCl (Black) or Isoproterenol (Iso) treatment (Red), normalized to tibia length (TL) or body weight (BW). (n≥7 per group) **D**, Representative images of echocardiographic M-mode (top) and Masson Trichrome staining (bottom). **E**, Time course of averaged fractional shortening (FS). (n≥7 per group) **F**, Time course of calculated left ventricular weight (LVW). (n≥7 per group) **G**, Mean heart rate measured during echocardiography before, 2 and 4 weeks after osmotic pumps implantation. (n≥7 per group) **H**, Mean of heart interstitial fibrosis area in WT or PDE4B-TG left ventricles of mice treated either with NaCl (Black) or Iso (Red). (n≥4 per group) Graphs represent the mean ± SEM. Statistical significance

was determined by Two-Way ANOVA *P<0.05, ***P<0.001, $ vs WT Iso, # vs WT NaCl.

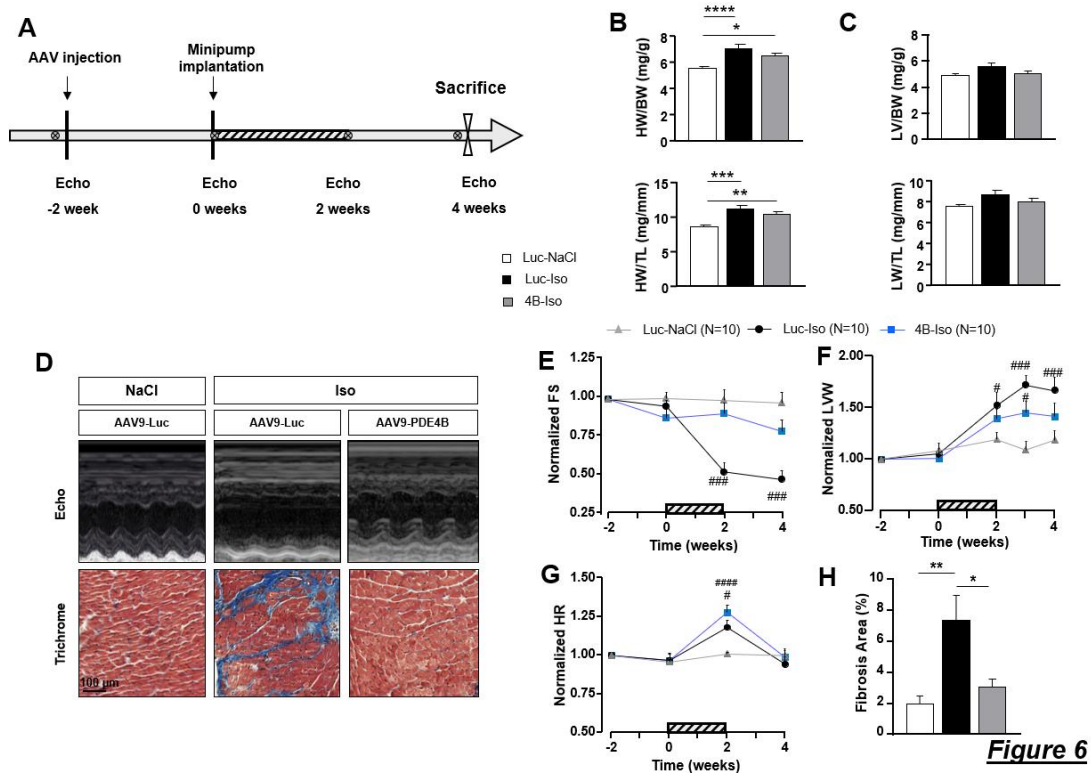

Figure 6: Gene therapy with PDE4B protects against maladaptive remodeling induced by chronic isoproterenol treatment.

A, Schematic representation of the chronic isoproterenol (Iso) infusion protocol. Mice were injected with either AAV9 encoding for luciferase (AAV9-Luc) or PDE4B (AAV9-PDE4B). Two weeks later, AAV9-Luc injected mice were implanted subcutaneously with osmotic minipumps diffusing 60 mg/Kg/day of Iso or vehicle solution (0.9% NaCl) during 2 weeks (hatched bars) while AAV9-PDE4B injected animals were implanted only with minipumps delivering Iso. Mice were kept alive for two additional weeks prior sacrifice. Cardiac function was evaluated by echocardiography before, 2 and 4 weeks after the minipump implantation. **B** and **C**, Mean heart (HW) and lung weight (LW) of AAV9-Luc mice treated with NaCl (Luc-NaCl, white bars) or Iso (Luc-Iso, black bars) and of AAV9-PDE4B mice treated with Iso (4B-Iso, grey bars), normalized to tibia length (TL) or body weight (BW). (n=10 per group) **D**, Representative images of echographic M-mode (top) and Masson Trichrome staining (bottom). **E**, Time course of averaged fractional shortening (FS). (n=10 per group) **F**, Time course of calculated left ventricular weight (LVW). (n=10 per group) **G**, Mean heart rate measured during echocardiography before, 2 and 4

weeks after osmotic pumps implantation. (n=10 per group) **H**, Mean of heart interstitial fibrosis area in left ventricles of Luc-NaCl, Luc-Iso or 4B-Iso mice. (n=10 per group) Graphs represent the mean ± SEM. Statistical significance was determined by One-Way and Two-Way ANOVA *P<0.05, **P<0.01, ***P<0.001, # vs WT NaCl.

Supplementary Figures and Tables

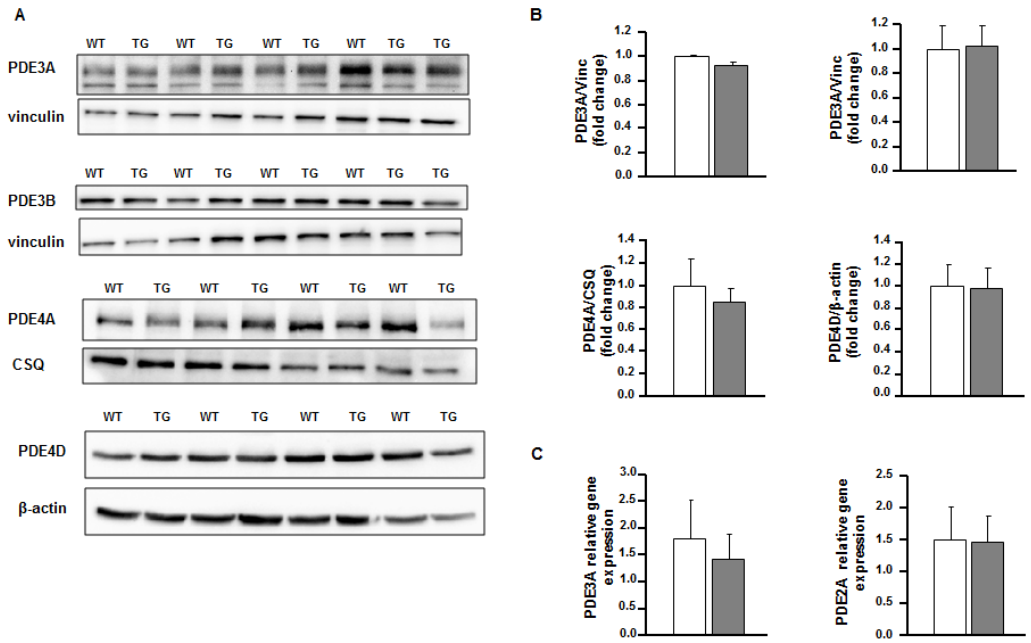

Figure S1

Figure S1: PDE4B-TG hearts don't show modifications in other main cardiac PDEs isoforms expression.

A, Representative westen blot images of isoforms of PDE3a, 3b, and PDE4a and 4d expression in cardiac lysates of WT ans TG mice. **B**, Western blot analysis of PDEs expression (n≥4 per group). Vinculin is used as normalizer (Vinc). **C**, Fold-changes in mRNA levels of PDE2a and PDE3a in cardiac lysates (n≥7 per group). Graphs represent the mean ± SEM. Statistical significance was determined by Student T-test.

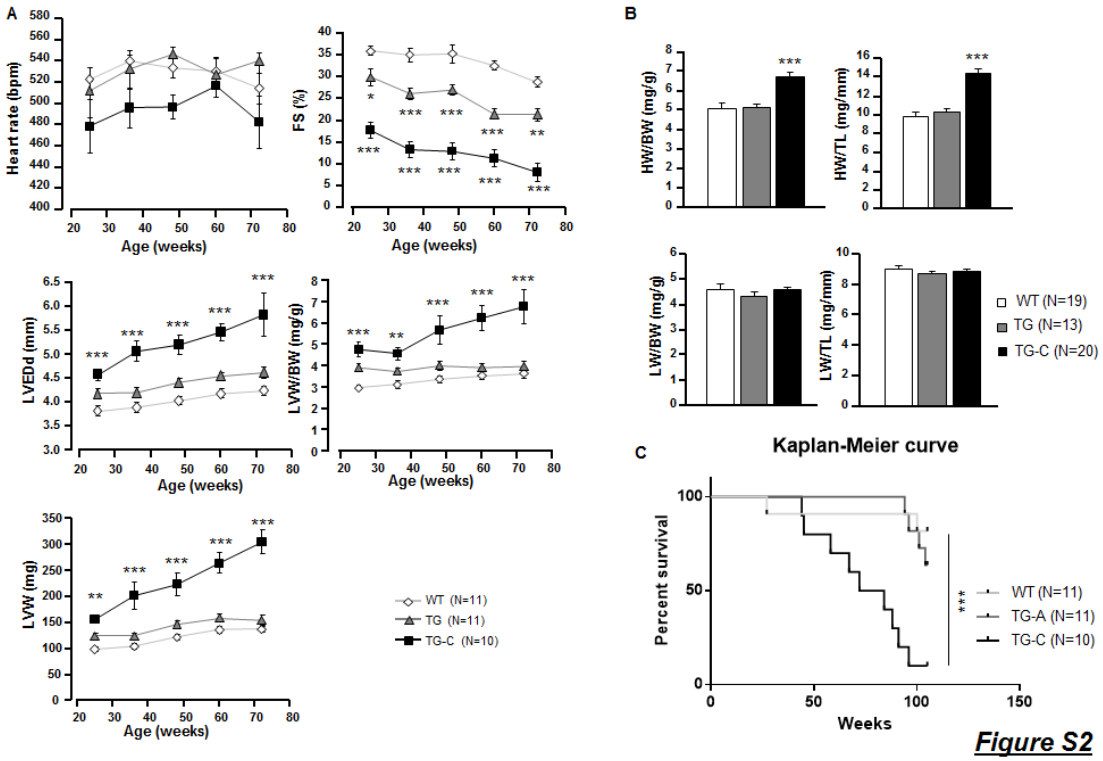

Figure S2: PDE4B overexpression does not alter mice survival during aging.

A, Time course of echographic parameters during aging on WT and TG mice (n=10-11 per group). **B**, Quantification of heart weight and lung weight to body weight or to tibia length ratios at 59.1 ±0.7 weeks of age (n≥13 per group). **C**, Kaplan-Meier curve showing WT and TG mice survival until 85 weeks of age (n=11 per group). Graphs represent the mean ± SEM. Statistical significance was determined by One-Way and Two-Way ANOVA **P*<0.05, ***P*<0.01, ****P*<0.001. Statistical significance for Kaplan-Meier curve was determined by Wilcoxon-Gehan test ****P*<0.001.

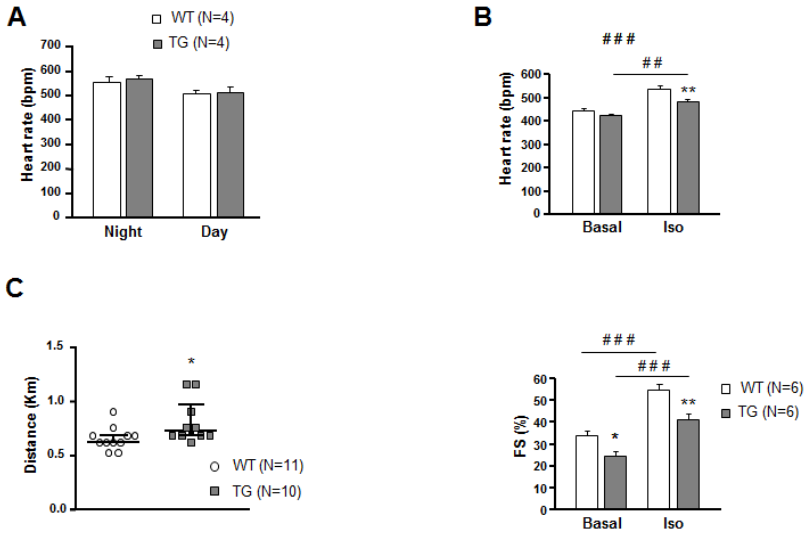

Figure S3

Figure S3: PDE4B-TG mice of heart function and physical exercise endurance.

A, Heart rate measured by ECG telemetry on vigile mice during 24 hours (n=4 per group). **B**, WT and TG mice were subjected to an intra-peritoneal Iso injection (0.02 mg/Kg); heart rate and fractional shortening (FS) were measured by 6-lead ECG and echocardiography respectively, at baseline and 2 minutes after injection, on anesthetized mice (n=6 per group). **C**, Endurance distance of treadmill running to exhaustion in WT and TG mice (n>9 per group). Graphs represent the mean ± SEM. Statistical significance was determined by Student T-test **P*<0.05, Two-Way ANOVA (WT vs TG) **P*<0.05, ***P*<0.01, (Basal vs Iso) ##*P*<0.01, ###*P*<0.001.

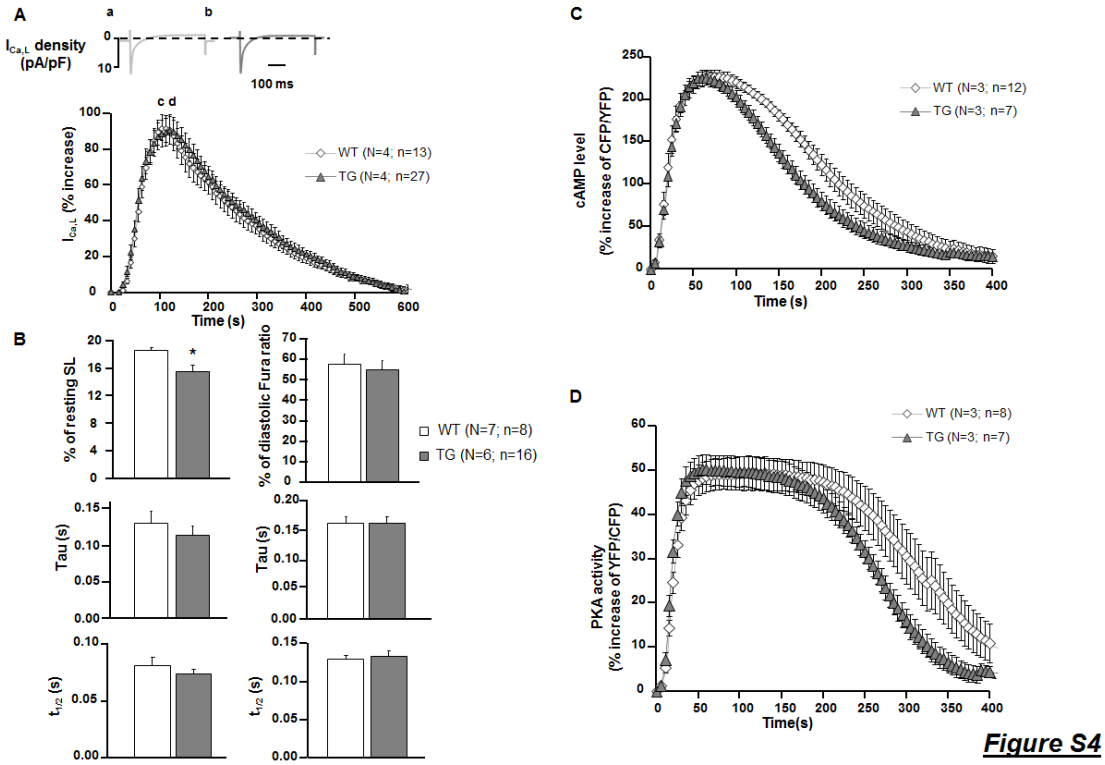

Figure S4: PDE4B inhibitor, Ro20-1724 (Ro), restores β-AR stimulation responses in TG to WT levels.

A, Typical traces obtained of $I_{Ca,L}$ current in a WT (a) and TG (b) cell at the maximum response to 15-second pulse of Iso (30 nM) + 10 µM Ro (top graph). Mean variation of $I_{Ca,L}$ after Iso (30nM, 15 s) and Ro (10µM) application (n=4; N≥16) (bottom graph). **B**, Mean variation of Sarcomere length (SL) and calcium transients amplitudes, and decay kinetics (Tau) of these parameters upon Iso (100nM) and Ro (10µM) application on ventricular myocytes loaded with 3µM Fura-2 AM probe, paced at 0.5 Hz, using an Ionoptix system (n≥6, N≥22). **C** and **D**, Mean variation of cAMP level and PKA activity upon 15-second pulse of Iso (30 nM) and Ro (10 µM) measured on FRET microscopy (n=3; N≥7 per group). Graphs represent the mean ± SEM. Statistical significance was determined by Student T-test **P*<0.05, and One-Way ANOVA .

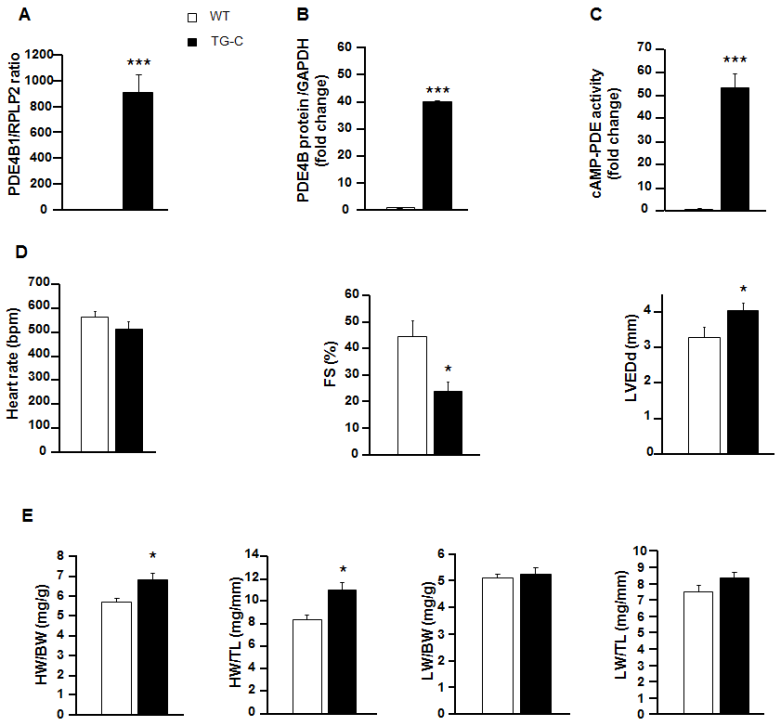

Figure S5

Figure S5: Strong cardiac specific overexpression of PDE4B leads to severe cardiac hypertrophy and drastically diminishes heart function leading to premature death.

A-C, PDE4B mRNA levels , protein levels, and PDE activity, were evaluated for up to 70 weeks. (n>7 per group) **D**, Mean values of heart rate, fractional shortening (FS), left ventricle end-diastolic diameter (LVEDd). (n>7 per group) **E**, Mean values of measured HW, and lung weight (LW) normalized to body weight (BW) and tibia length (TL) obtained from WT, TG-C mice. (n>7 per group) Graphs represent the mean ± SEM. Statistical significance was determined by Student T-test **P*<0.05, ****P*<0.001.

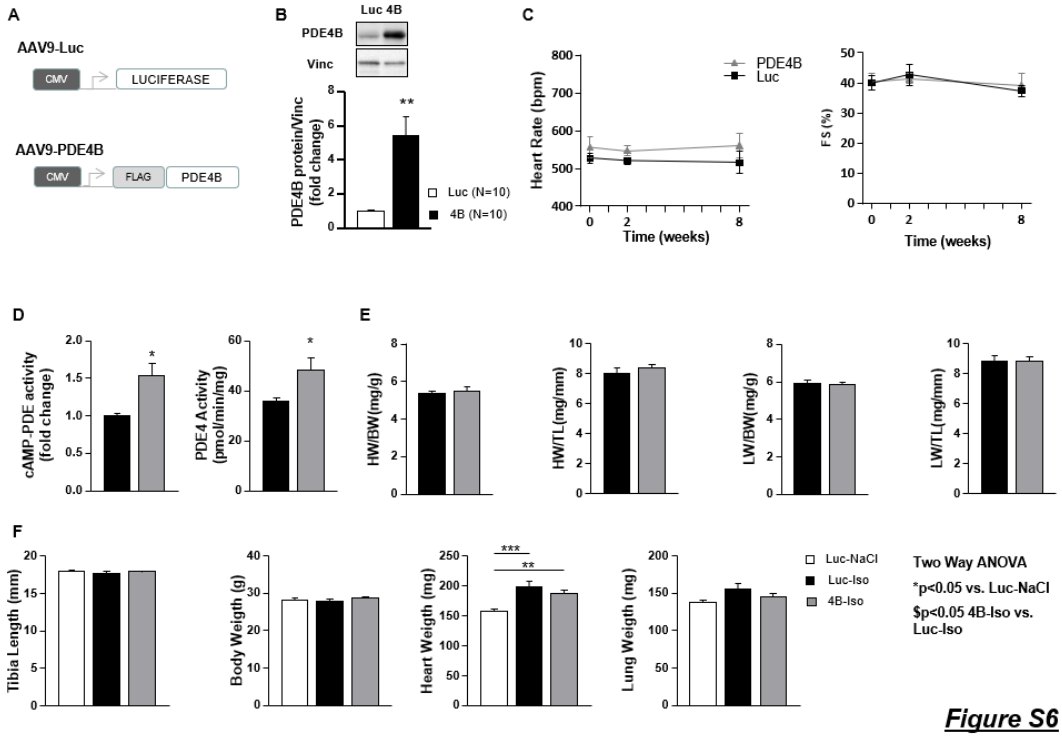

Figure S6: PDE4B overexpression by AAV9 does not affect physiological heart function.

A, Schematic representation of the constructions used to produce the adeno-associated viruses. Both viruses express the protein of interest downstream of cytomegalovirus promoter (CMV). AAV9-Luc expresses the Luciferase (Luc) protein and is used as a control, AAV9-PDE4B (4B) expresses the longest isoform of PDE4B (NM_019840.2) fused with a FLAG-tag (MDYKDDDDK) at the N-terminal. **B**, PDE4B protein expression in heart extracts measured by Western blot. (n=10 per group) Vinculin is used as nomalizer (Vinc). **C**, Time course analysis of heart rate and fractional shortening measured by echography in mice. (n=4 per group). **D**, PDE and PDE4 specific activity was measured in mice ventricular protein extracts. (n=4 per group) **E**, Quantification of heart weight and lung weight, over body weight and tibia length ratios, in physiological conditions. (n=4 per group). **F**, Quantification of body weight, tibia length, heart weight, lung weight, in Isoproterenol treated mice. (n≥9 per group). Graphs represent the mean ± SEM. Statistical significance was determined by Student T-test **P*<0.05, One-Way and Two-Way ANOVA ***P*<0.01, ****P*<0.001.

Supplementary Table 1. Cardiac parmeters in Iso treated WT and TG mice.

	WT-Nacl			WT-Iso			TG-Nacl			TG-Iso		
	Mean	sem	N	Mean	sem	N	Mean	sem	N	Mean	sem	N
HW (mg)	173	6	8	209 $	7	9	203	12	9	207	15	7
LW (mg)	150	3	8	174 $	8	9	152	4	9	161	10	7
BW (g)	27.6	0.6	8	28.3	0.7	9	28.2	0,5	9	27.4	1,0	7
TL (mm)	17.9	0.2	8	17.9	0.1	9	18.1	0.1	9	17.6	0.2	7
HW/BW (mg/g)	6.2	0.1	8	7.4 $	0.3	9	7.2	0.3	9	7.5	0.3	7
HW/TL (mg/mm)	9.6	0.3	8	11.7 $	0.4	9	11.2	0.7	9	11.7	0.8	7
LW/BW (mg/g)	5.4	0.1	8	6.2	0.3	9	5.4	0.1	9	5.9	0.4	7
LW/TL (mg/mm)	8.4	0.1	8	9.8 $	0.4	9	8.4	0.2	9	9.2	0.6	7

Two Way ANOVA
#p<0.05 TG ISO vs. WT ISO
$p<0.05 WT ISO vs. WT NaCl
*p<0.05 TG ISO vs. TG NaCl

Table S1

Table S1: protection against maladaptive remodeling induced by chronic infusion with isoproterenol in PDE4B-TG mice.

A, Anatomical parameters measured at the time of sacrifice in WT and TG adult mice treated with either NaCl or Iso for two weeks. Statistical significance was determined by Two-Way ANOVA (WT Iso vs TG Iso) #$P<0.05$, (WT Iso vs WT NaCl) $ $P<0.05$, (TG Iso vs TG NaCl) * $P<0.05$.

Methods and Materials

All experiments were carried out according to the European Community guiding principles in the care and use of animals (2010/63/UE, 22 september 2010), the local Ethics Committee (CREEA Ile-de-France Sud) guidelines and the French decree n° 2013-118, 1st February 2013 on the protection of animals used for scientific purposes (JORF n°0032, 7 February 2013 p2199, text n° 24).

Transgenic mouse generation.
Mice overexpressing PDE4B specifically in the heart (PDE4B-TG) were generated at the Institut Clinique de la Souris (Strasbourg, France). Mouse PDE4B3 cDNA (a kind gift from Dr. J. Cherry, Boston University, Boston, MA)[1] was subcloned into a pBluescript-based vector between the 5.5-kb murine α-MHC promoter and the human growth hormone polyadenylation sequence (a kind gift from Dr J. Robbins, Children's Hospital Research Foundation, Cincinnati, Ohio).[2] The purified transgene fragment was injected into pronuclei of a fertilized mouse eggs and the injected eggs were surgically implanted into pseudopregnant females. Genotype of mouse pups was confirmed by PCR assay.

Preparation of mouse ventricular myocytes.
Mice were anesthetized by intraperitoneal injection of pentothal (150 mg/kg), and the heart was quickly removed and placed into a cold Ca^{2+}-free Tyrode's solution containing 113 mM NaCl, 4.7 mM KCl, 1.2 mM MgSO4-7H2O, 0.6 mM KH2PO4, 0.6 mM NaH2PO4, 1.6 mM NaHCO3, 10 mM HEPES, 30 mM Taurine, and 20 mM glucose, adjusted to pH 7.4. The ascending aorta was cannulated, and the heart was perfused with oxygenated Ca^{2+}-free Tyrode's solution at 37°C for 4 minutes using retrograde Langendorff perfusion. For enzymatic dissociation, the heart was perfused with Ca2+-free Tyrode's solution containing LiberaseTM Research Grade (Roche Diagnostics) for 10 minutes at 37°C. Then the heart was removed and placed into a dish containing Tyrode's solution supplemented with 0.2 mM $CaCl_2$ and 5 mg/ml BSA (Sigma-Aldrich). The ventricles were separated from the atria, cut into small pieces, and triturated with a pipette to disperse the myocytes. Ventricular myocytes were filtered on gauze and allowed to sediment by gravity for 10 minutes. The supernatant was removed, and cells were suspended in Tyrode's solution supplemented with 0.5 mM $CaCl_2$ and 5 mg/ml BSA. Cells were suspended in Tyrode's solution with 1 mM $CaCl_2$. For $I_{Ca,L}$ recording and Ionoptix experiments, freshly isolated ventricular myocytes were plated in 35-mm culture dishes coated with laminin (10 μg/ml) and stored at room temperature until use. For primary culture, Tyrode's solution was replaced by Minimum Essential Medium (MEM, 51200, Gibco) supplemented with 5% FBS, 2% penicillin-streptomycin, 0.1% BSA, 2 mM L-glutamine, Insulin Transferin Selenium 1X and plated on 35 mm culture dishes coated with laminin (10 μg/ml) at a density of 10^4 cells per dish. AMVMs were left to adhere for 2 h in a 95% O_2, 5% CO_2 atmosphere at 37°C, before the medium was replaced with FBS-free MEM containing adenoviruses encoding the cAMP FRET

sensor Epac-S^{H187} [20,22]or the cytoplasmic PKA sensor AKAR3-NES[21,26] at a multiplicity of infection of 1000 active viral particles per cell for 24 h. Viability of cardiomyocytes was confirmed during the experiment by checking their shape.

AAV9 vector production, purification and characterization

AAV9-PDE4B carries a PDE4B expression cassette flanked by two AAV2 inverted terminal repeats. The expression sequence is pseudotyped with an AAV9 capsid. The PDE4B3 expression cassette contains a CMV promoter, a β-globin intron, the murine PDE4B coding sequence and a hGH polyadenylation signal. AAV9-4B was produced in AAV-293T cells (Stratagene #240073) with the three-plasmid method and Calcium-Chloride transfection. The virus was purified by Cesium-Chloride gradient. Viral particle titers were determined by Real Time PCR on the CMV promoter. For control condition, an expression cassette encoding firefly luciferase under the control of a CMV promoter was packaged into AAV9 capsids and purified on Cesium-Chloride gradient to yield AAV9-Luc virus. The average concentrations obtained for both viruses were 4-5x10^{12} vp/ml, thus allowing a single tail vein injection of 200-250 µl of viral solution for each mouse, corresponding to 1x10^{12} vp per mouse. The efficiency of transduction was assessed by western blot analysis of ventricular tissue. We assumed uniform transduction of the virus throughout the heart as previously published[27].

Reagents.

Ro 20-1724 (Ro) was from Calbiochem (San Diego, USA).

Transthoracic echocardiography.

Transthoracic two-dimensional-guided M-mode echocardiography of mice was performed using an echocardiograph with a 15 MHz Linear transducer (Vivid 9, General Electric Healthcare, Vélizy Villacoublay, France) under 3% isoflurane gas anaesthesia. Heart rate was monitored during echocardiography and only traces with heart rate greater than 450 beat per minute were counted. All the measures were taken using the papillary muscle as anatomical reference. Wall thickness and left ventricular chamber dimensions in systole and diastole were determined and used to calculate left ventricle Fractional Shortening (FS) and Ejection Fraction (EF). Ejection Fraction measures were not shown in this study as they are derived from the same echocardiographic parameters used to calculate FS, therefore giving exactly the same results. Left ventricular mass (LVM) was calculated according to the Penn formula assuming a spherical LV geometry and validated for the rat heart ($LVM=1.04\times[(LVTDd+IVS+PW)^3-(LVTDd)^3]$, where 1.04 is the specific gravity of muscle, LVTDd is left ventricular telediastolic diameter, IVS and PW are end-diastolic interventricular septum and posterior wall thicknesses. The analysis was not performed blind.

Perfused heart preparation.

Male mice (PDE4B-TG and WT littermates) were anaesthetized with intraperitoneal

injection of pentobarbital (150 mg/kg). The heart was quickly removed and placed into a solution for dissection containing (in mM): NaCl 116, D-glucose 15, $NaHCO_3$ 25, KCl 4.7, KH_2PO_4 1.2, $MgSO_4$ 1.2, $CaCl_2$ 0.4, at 4°C, oxygenated (95% O_2–5% CO_2). Then, the aorta was cannulated and perfused by the Langendorff method with Krebs-Henseleit solution containing (in mM): NaCl 116, D-glucose 11, $NaHCO_3$ 25, KCl 4.7, KH_2PO_4 1.2, $MgSO_4$ 1.2, $CaCl_2$ 1.2, Pyruvate 2, EDTA 0.1, at a constant pressure of 75 mm Hg and a temperature of 37.0±0.5°C. A latex balloon filled with water and ethanol (90/10) connected to a pressure transducer (Statham gauge Ohmeda, Bilthoven, The Netherlands) was introduced into the left ventricle after crossing the mitral valve. For each heart, the experiment started with a progressive increase of the latex balloon inserted inside the left ventricle to generate a ventricular volume-developed pressure relationship. When the maximal developed pressure was reached, ten minutes of equilibration in isovolumic working conditions were imposed before measuring cardiac parameters. Heart rate, left ventricular developed pressure (LVDP) and the first derivatives of LV pressure (LV +dP/dtmax and LV -dP/dtmax) were measured online using a dedicated software (Emka technologies data analyzer, Paris, France). Then, the hearts were paced at 650 bpm using platinum electrode placed on the surface of the right ventricle and increasing concentrations of isoprenaline (Iso) were infused from 0,1 nM to 100 nM. Pacing was stopped in the presence of 100 nM Iso to record spontaneous cardiac parameters.

Isoprenaline infusion model.

Mice (25–30g) at 10-weeks of age were treated for 14 days with either isoprenaline (60 mg/kg/day, Iso, Sigma St. Louis, MO, USA) or vehicle (0.9% NaCl, Ctr) administered via osmotic minipumps (2002, Alzet, USA). Two weeks after the end of the treatment, animal were anesthetized by intraperitoneal injection of pentothal (150 mg/Kg). Hearts were rapidly removed and remaining blood was washed out in cold Ca^{2+}-free KREBS solution (120 mM NaCl, 4.8 mM KCl, 2.4 mM $MgSO_4$-7H2O, 1.2 mM KH_2PO_4 and 24 mM $NaHCO_3$). Transversal slice of 3-4 mm of width was cut in the middle of the heart and rapidly fixed in 4% paraformaldehyde for histology. The rest of ventricular tissue was frozen in liquid nitrogen and stored at -80°C until use.

Preparation of protein extracts.

For PDE assay, frozen adult mouse hearts were homogenized in ice-cold buffer containing (in mM): NaCl 150, HEPES 20 (pH 7.4), EDTA 2, and supplemented with 10% glycerol, 0.5% NP-40, 1 μM microcystin-LR, and Complete Protease Inhibitor Tablets (Roche Diagnostics). Tissue lysates were centrifuged at 3,000 g and 4°C for 10 minutes, and supernatants were used. For western blotting, frozen cardiac tissues were homogenized in a RIPA buffer containing (in mM): NaCl (150, Tris-HCl 50 (pH 7.4), EDTA 2, and supplemented with 1% NP-40, 0.1% SDS, 1% Deoxycholate, Complete Protease Inhibitor Tablets and PhosSTOP™ phosphatase inhibitor tablets (Roche Diagnostics). Tissue lysates were centrifuged at 15,000 g and 4°C for 20 minutes, and supernatants were used.

PDE activity assay.

Cyclic AMP-PDE activity was measured according to the method of Thompson and Appleman[3] as described previously.[4] In brief, samples were assayed in a 200-μL reaction mixture containing 40 mM Tris-HCl (pH 8.0), 1 mM $MgCl_2$, 1.4 mM β-mercaptoethanol, 1 μM cAMP, 0.75 mg/ml bovine serum albumin, and 0.1 μCi of [^{3}H]cAMP for 30 minutes at 33°C. The reaction was terminated by heat inactivation in a boiling water bath for 1 minute. The PDE reaction product 5′-AMP was then hydrolyzed by incubation of the assay mixture with 50 μg Crotalus atrox snake venom for 20 minutes at 33°C, and the resulting adenosine was separated by anion exchange chromatography using 1 ml AG1-X8 resin (Bio-Rad) and quantified by scintillation counting.

Western blot analysis.

Protein samples were separated in denaturating acrylamide gels and subsequently transferred onto PVDF membranes. After blocking the membranes with 5% milk buffer for 1 h, the incubation with primary antibodies was carried out over night at 4°C. After incubation with appropriate secondary antibodies for 1 h, proteins were visualized by enhanced chemoluminescence and quantified with Quantity One software.

The primary antibodies used were: rabbit anti-PDE4B (113-4) raised against the C-terminus of PDE4B, rabbit anti-PDE4A (AC55), mouse anti-PDE4D (ICOS) (the three being kind gifts from Dr. Marco Conti, UCSF, California, USA), anti-phospholamban (PLB) (sc-21923, Santa Cruz), anti-p-PLB (Thr17) (A010-13, Badrilla), anti-p-PLB (Ser16) (A010-12, Badrilla), anti-troponin I (TnI) (4002, Cell Signaling), anti-p-TnI (Ser22-23) (4004, Cell Signaling), anti-myosin-binding protein C (MyBPC3) (sc-50115, Santa Cruz), anti-p-MyBPC3 (Ser282) (ALX-215-057-R050, Alexis), rabbit anti-PDE3A (a kind gift from Dr C. Yan, University of Rochester, Rochester, NY, USA), rabbit anti-PDE3B (a kind gift from Dr A. Ghigo and E. Hirsch, University of Torino, Torino, Italy), mouse anti-β-actin (sc-47778, Santa Cruz), anti-calsequestrin (CSQ) (PA1-193, Pierce), mouse anti-vinculin (Vinc) (V9131, Sigma). Different housekeeping genes were used for different experiments in order to avoid membrane stripping.

$I_{Ca,L}$ current measurements.

The whole-cell configuration of the patch-clamp technique was used to record $I_{Ca,L}$. Patch electrodes with 1–2 MΩ resistance when filled with internal solution contained 118 mM CsCl, 5 mM EGTA, 4 mM $MgCl_2$, 5 mM sodium phosphocreatine, 3.1 mM Na_2ATP, 0.42 mM Na_2GTP, 0.062 mM $CaCl_2$ (pCa 8.5), and 10 mM HEPES, adjusted to pH 7.3. External Cs^+-Ringer solution contained 107.1 mM NaCl, 20 mM CsCl, 4 mM $NaHCO_3$, 0.8 mM NaH_2PO_4, 5 mM glucose, 5 mM Na pyruvate, 10 mM HEPES, 1.8 mM $MgCl_2$, and 1.8 mM $CaCl_2$, adjusted to pH 7.4. The cells were depolarized every 8 seconds from –50 mV to 0 mV for 400 ms. The use of –50 mV as holding potential allowed the inactivation of voltage-dependent sodium currents. Potassium currents were blocked by replacing all K^+ ions with external and internal Cs^+.

Viability of cardiomyocytes was confirmed during the experiment by checking their shape.

Measurements of Ca^{2+} transients and cell shortening.

Isolated cardiomyocytes were loaded with 3 μM Fura-2 AM (Invitrogen) at room temperature for 15 minutes and then washed with external Ringer solution containing (in mM): NaCl 121.6, KCl 5.4, $NaHCO_3$ 4.013, NaH_2PO_4 0.8, 10 mM HEPES, glucose 5, Na pyruvate 5, $MgCl_2$ 1.8, and $CaCl_2$ 1, pH 7.4. Viability of cardiomyocytes was confirmed during the experiment by checking their shape. The loaded cells were field stimulated (5 V, 4 ms) at a frequency of 0.5 Hz. Sarcomere length (SL) and Fura-2 ratio (measured at 512 nm upon excitation at 340 nm and 380 nm) were simultaneously recorded using an IonOptix System (IonOptix). Cell contractility was assessed by the percentage of sarcomere shortening, which is the ratio of twitch amplitude (difference of end-diastolic and peak systolic SL) to end-diastolic SL. Ca^{2+} transients were assessed by the percentage of variation of the Fura-2 ratio by dividing the twitch amplitude (difference of end-diastolic and peak systolic ratios) to end-diastolic ratio. The Tau was used as an index of relaxation and Ca^{2+} transient decay kinetics. All parameters were calculated offline using a dedicated software (IonWizard 6x).

Cyclic AMP level and PKA activity measurements by fluorescent resonance energy transfer (FRET) imaging.

Freshly isolated ventricular myocytes from PDE4B-TG and WT mice were infected with adenoviruses to measure cAMP and PKA activity, respectively. Viability of cardiomyocytes was confirmed during the experiment by checking their shape. The cells were then washed once and maintained in the Ringer solution described above containing 1.8 mM $CaCl_2$, at room temperature, Images were captured every 5 seconds using the 40× oil immersion objective of an inverted microscope (Nikon) connected to a software-controlled (Metafluor, Molecular Devices) cooled charge coupled (CCD) camera (Cool SNAP HQ2). CFP was excited during 300 ms by a Xenon lamp (100W, Nikon) using a 440/20BP filter and a 455LP dichroic mirror. Dual emission imaging of CFP and YFP was performed using a Dual-View emission splitter equipped with a 510LP dichroic mirror and 480/30 nm, 535/25 nm BP filters. Average fluorescence intensity was measured in a region of interest comprising the entire cell. Background was subtracted and CFP bleed through in the YFP channel was corrected before calculating the YFP/CFP ratio for the AKAR3-NES sensor or the CFP/YFP ratio for the Epac-S^{H187} sensor. Ratio images were obtained using Image J software.

Histology

Hearts were fixed in 4% paraformaldehyde and then embedded in paraffin. Paraffin sections (5 μm) were stained with Masson's trichrome kit (Microm, France). Slides were scanned by the digital slide scanner NanoZoomer 2.0-RS (Hamamatsu) allowing an overall view of the samples. Images were digitally captured from the scanned

slides using the NDP.view2 software (Hamamatsu). Fibrosis analysis was performed by quantifying the blue area over the total area of the image using ImageJ. Fibrosis percentage was not normalized on the area of the left ventricular section. Tha analysis was performed blind.

Statistics

All results are expressed as mean±SEM and were analyzed using the GraphPad Prism software (GraphPad software, Inc., La Jolla, CA, USA). Normal distribution was tested by the Shapiro-Wilk normality test. For simple two-group comparison, we used an unpaired Student t-test or a Mann-Whitney test when the data did not follow a normal distribution. Differences between multiple groups were analyzed using an ordinary one-way ANOVA with Tukey's multiple comparisons post-hoc test, or a Kruskal Wallis with Dunn's multiple comparisons post-hoc test, when the data did not follow a normal distribution. A two-way ANOVA and Tukey's or Sidak's multiple comparisons post-hoc test was used when appropriate. Differences with P-values <0.05 were considered as statistically significant.

Acknowledgements

First and foremost I want to sincerely thank my advisors Prof. Jerome Leroy, Dr. Gregoire Vandecasteele and Dr. Rodolphe Fischmeister. Prof. Leroy has guided and trained me, not only on how to perform a rigorous experiment but also on what the right attitude to science has to be. I learned plenty of skills and spirits from him. I appreciate all his contributions of ideas, time and patient to make my PhD work meaningful and productive. I also sincerely thank Dr. Gregoire Vandecasteele and Dr. Rodolphe Fischmeister for giving me the chance to work in the lab. Their smart, courtesy and rigorousness always inspired me. They gave me a great deal of chances to read and to improve my knowledge in the field. The discussions and feedback from them has made my Ph.D. work progress well.

I would like to thank the members of the laboratory in Turin who contributed to this work, in particular Prof. Alessandra Ghigo, Prof. Emilio Hirsch, Prof. Emilia Turco, Dr. Fiorella Balzac, and Dr. Cristina Rubinetto who contributed to the successfulness of experiments using adeno-associated virus.

I would like to thank the members of the laboratory in Nantes who contributed to this work, in particular Prof. Flavien Charpentier and Agnès Hivonnait for their contribution in the understanding of arrhythmic events.

I would like to thank my colleagues who had helped me with the experimental work. Dr. Sarah Karam, Dr. Marta Lindner and Dr. Ibrahim Bedioune helped me a lot with the cardiac experiments and I had very useful discussions with them. Délphine Mika and Hind Mehel shared with me their expertise in phosphodiesterases. Jerome Vinck helped me during the validation of the luciferase activity and in experiments troubleshooting. I want to thank Sarah Idres, Audrey Varin and Guillaume Pidoux for the useful hints on cellular biology experiments. I also want to thank Liang Zhang for his help during PDE activity measurement and useful discussions on PDE inhibitors. Fiona Bartoli, Maxence Ribeiro, Carole Oudot, Mélanie Gressette, Julie Pires Da Silva and Lucile Grimbert for their help during cellular biology experiments. This research work would not have progressed without their collaboration and team work.

I gratefully acknowledge the funding supports from Università Italo-Francese (UIF) which made my PhD work possible.

References

1. Ponikowski, P. *et al.* 2016 ESC Guidelines for the diagnosis and treatment of acute and chronic heart failure. *Eur. Heart J.* **37,** 2129–2200 (2016).
2. Breckenridge, R. Heart failure and mouse models. *Dis. Model. Mech.* **3,** 138–43 (2010).
3. Balazs, T. & Herman, E. H. Toxic cardiomyopathies. *Ann. Clin. Lab. Sci.* **6,** 467–76 (1976).
4. Kim, G. E. & Kass, D. A. Cardiac Phosphodiesterases and Their Modulation for Treating Heart Disease. in *Handbook of experimental pharmacology* **243,** 249–269 (2016).
5. Lugnier, C. Cyclic nucleotide phosphodiesterase (PDE) superfamily: A new target for the development of specific therapeutic agents. *Pharmacol. Ther.* **109,** 366–398 (2006).
6. Bobin, P. *et al.* Cyclic nucleotide phosphodiesterases in heart and vessels: A therapeutic perspective Phosphodiestérases des nucléotides cycliques dans le coeur et les vaisseaux : une perspective thérapeutique. *Arch. Cardiovasc. Dis.* **109,** 431–443 (2016).
7. Turnham, R. E. & Scott, J. D. Gene Wiki Review Protein kinase A catalytic subunit isoform PRKACA; History, function and physiology. *Gene* **577,** 101–108 (2016).

8. Bender, A. T. & Beavo, J. A. Cyclic nucleotide phosphodiesterases: molecular regulation to clinical use. *Pharmacol. Rev.* **58,** 488–520 (2006).

9. Jin, S.-L. C., Lan, L., Zoudilova, M. & Conti, M. Specific role of phosphodiesterase 4B in lipopolysaccharide-induced signaling in mouse macrophages. *J. Immunol.* **175,** 1523–31 (2005).

10. Jin, S. L., Richard, F. J., Kuo, W. P., D'Ercole, A. J. & Conti, M. Impaired growth and fertility of cAMP-specific phosphodiesterase PDE4D-deficient mice. *Proc. Natl. Acad. Sci. U. S. A.* **96,** 11998–2003 (1999).

11. Jin, S.-L. C., Latour, A. M. & Conti, M. Generation of PDE4 Knockout Mice by Gene Targeting. in *Phosphodiesterase Methods and Protocols* 191–210 (Humana Press, 2005). doi:10.1385/1-59259-839-0:191

12. Jin, S.-L. C. & Conti, M. Induction of the cyclic nucleotide phosphodiesterase PDE4B is essential for LPS-activated TNF-alpha responses. *Proc. Natl. Acad. Sci. U. S. A.* **99,** 7628–33 (2002).

13. Packer, M. *et al.* Effect of Oral Milrinone on Mortality in Severe Chronic Heart Failure. *N. Engl. J. Med.* **325,** 1468–1475 (1991).

14. Rochais, F. *et al.* A specific pattern of phosphodiesterases controls the cAMP signals generated by different Gs-coupled receptors in adult rat ventricular myocytes. *Circ. Res.* **98,** 1081–8 (2006).

15. Mongillo, M. *et al.* Fluorescence resonance energy transfer-based analysis of cAMP dynamics in live neonatal rat cardiac myocytes reveals distinct functions of compartmentalized phosphodiesterases. *Circ. Res.* **95,** 67–75 (2004).

16. Leroy, J. *et al.* Phosphodiesterase 4B in the cardiac L-type Ca 2 + channel complex regulates Ca 2 + current and protects against ventricular arrhythmias in mice. *J. Clin. Invest.* **121,** 2651–2661 (2011).

17. Abi-Gerges, A. *et al.* Decreased expression and activity of cAMP phosphodiesterases in cardiac hypertrophy and its impact on β-Adrenergic cAMP signals. *Circ. Res.* **105,** 784–792 (2009).

18. Ghigo, A. *et al.* Phosphoinositide 3-Kinase γ Protects Against Catecholamine-Induced Ventricular Arrhythmia Through Protein Kinase A–Mediated Regulation of Distinct Phosphodiesterases. *Circulation* **126,** 2073–2083 (2012).

19. Mika, D., Richter, W., Westenbroek, R. E., Catterall, W. A. & Conti, M. PDE4B mediates local feedback regulation of β_1-adrenergic cAMP signaling in a sarcolemmal compartment of cardiac myocytes. *J. Cell Sci.* **127,** 1033–42 (2014).

20. Klarenbeek, J., Goedhart, J., van Batenburg, A., Groenewald, D. & Jalink, K. Fourth-Generation Epac-Based FRET Sensors for cAMP Feature Exceptional Brightness, Photostability and Dynamic Range:

Characterization of Dedicated Sensors for FLIM, for Ratiometry and with High Affinity. *PLoS One* **10,** e0122513 (2015).

21. Allen, M. D. & Zhang, J. Subcellular dynamics of protein kinase A activity visualized by FRET-based reporters. (2006). doi:10.1016/j.bbrc.2006.07.136

22. Vettel, C. *et al.* Phosphodiesterase 2 Protects Against Catecholamine-Induced Arrhythmia and Preserves Contractile Function After Myocardial Infarction. *Circ. Res.* **120,** 120–132 (2017).

23. Amieux, P. S. *et al.* Increased basal cAMP-dependent protein kinase activity inhibits the formation of mesoderm-derived structures in the developing mouse embryo. *J. Biol. Chem.* **277,** 27294–304 (2002).

24. Benjamin, I. J. *et al.* Isoproterenol-induced myocardial fibrosis in relation to myocyte necrosis. *Circ. Res.* **65,** 657–70 (1989).

25. Podetz-Pedersen, K. M., Vezys, V., Somia, N. V, Russell, S. J. & Mcivor, R. S. Cellular Immune Response Against Firefly Luciferase After Sleeping Beauty–Mediated Gene Transfer In Vivo. doi:10.1089/hum.2014.048

26. Haj Slimane, Z. *et al.* Control of cytoplasmic and nuclear protein kinase A by phosphodiesterases and phosphatases in cardiac myocytes. *Cardiovasc. Res.* **102,** 97–106 (2014).

27. Inagaki, K. *et al.* Robust systemic transduction with AAV9 vectors in mice: efficient global cardiac gene transfer superior to that of AAV8. *Mol. Ther.* **14,** 45–53 (2006).